Supplementary Figure 1

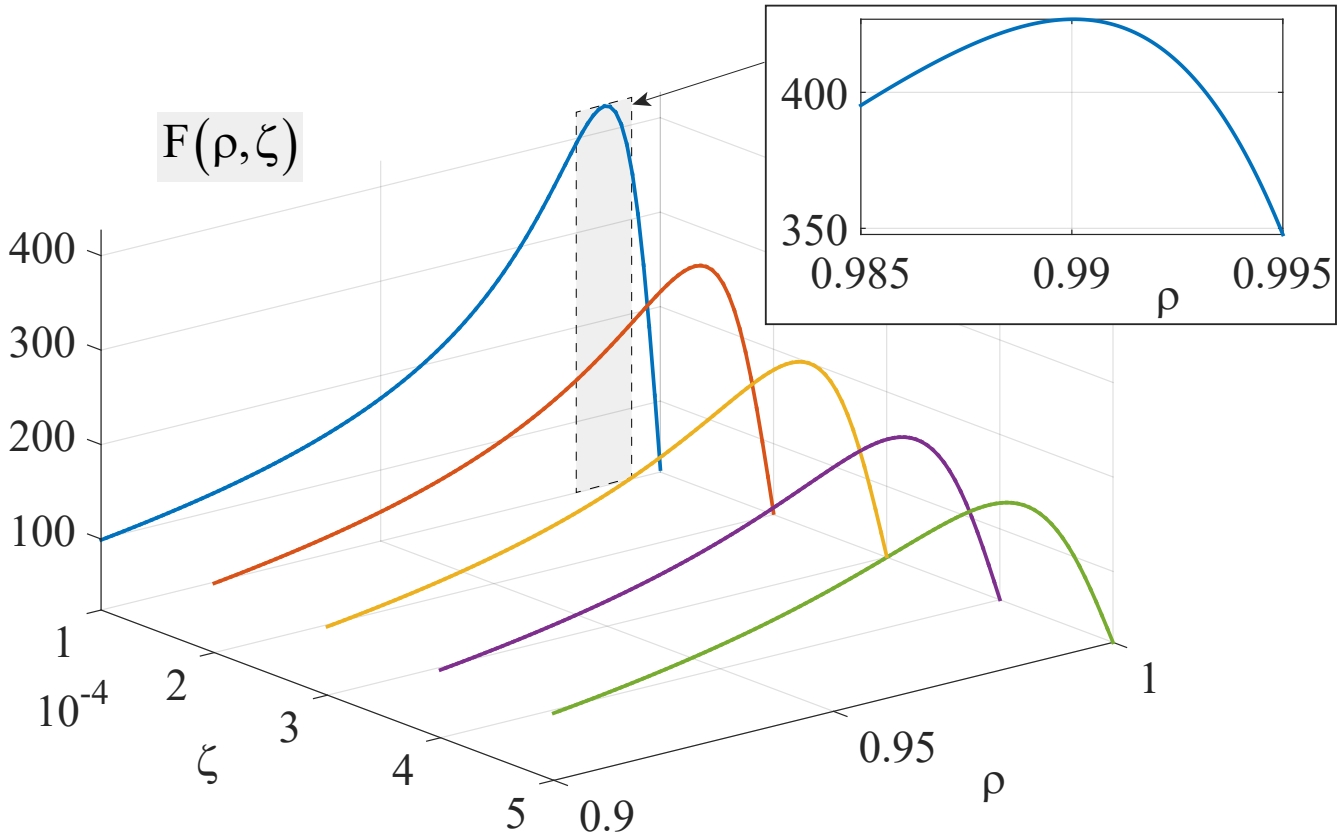

Supplementary Figure 1: Spatial dependence of the left-hand circular component of the field scattered by the graphene ring close to its inner edge (at $r_\perp = a$). The normalized spatial coordinates are $\rho = r_\perp/a$ and $\zeta = z/a$.

Supplementary Note 1

Graphene electromagnetic response. The graphene electromagnetic response at optical and infrared frequencies is dominated by the conical band structure $\mathcal{E} = \pm v_{\rm F} p$ around the two Dirac points, where $v_{\rm F} \approx 10^6$ m/s is the Fermi velocity and $\mathcal{E}, \mathbf{p}$ are the electron energy and momentum, respectively [1]. While in undoped graphene the Fermi energy lies at the Dirac points, injection of charge carriers through electrical gating [2] or chemical doping [3] shifts efficiently the Fermi level up to $E_{\rm F} \approx 1 - 2$ eV . Thus, within the photon energy range $\hbar\omega < 2E_{\rm F}$, where $\hbar$ is the reduced Planck constant, interband transitions are inhibited by the Pauli exclusion principle and graphene behaves like a 2D metal [4] with long relaxation time $\tau = \mu E_{\rm F}/ev_{\rm F}^2$ (μ is the electron mobility, which we set to the realistic value of $\mu = 1{\rm m}^2{\rm V}^{-1}{\rm s}^{-1}$ in our calculations) that can reach the picosecond time scale at moderate doping and purity both affecting the electron mobility [5]. In principle the graphene surface conductivity $\sigma(\mathbf{k}_\perp, \omega)$ is nonlocal and depends on the in-plane radiation wavevector $\mathbf{k}_\perp$. However, when $k_\perp < k_{\rm F} = E_{\rm F}/\hbar v_{\rm F}$ electron dynamics is local and the graphene conductivity can be evaluated within the local random phase approximation (RPA) providing the integral expression

$$\sigma(\omega) = \frac{-ie^2}{\pi\hbar^2(\omega + i/\tau)} \int_{-\infty}^{+\infty} d\mathcal{E} \left\{ |\mathcal{E}| \frac{\partial f_\mathcal{E}}{\partial \mathcal{E}} + \frac{f_\mathcal{E}\mathcal{E}/|\mathcal{E}|}{1 - 4\mathcal{E}^2/[\hbar(\omega + i/\tau)]^2} \right\}, \tag{1}$$

where $f_\mathcal{E} = \{1 + \exp[-(\mathcal{E} - E_{\rm F})/k_{\rm B}T]\}$ is the Fermi-Dirac occupation density of states up to the Fermi energy $E_{\rm F}$, $k_{\rm B}$ is the Boltzmann constant and T is the electron temperature.

Scattering in the long-wavelength limit. Consider the scattering of a monochromatic plane wave $\mathsf{E}^{(\rm i)}(\mathbf{r}, t) = {\rm Re}\left[\mathbf{E}^{(\rm i)}(\mathbf{r})\, e^{-i\omega t}\right]$ of amplitude $\mathbf{E}^{(\rm i)} = \mathbf{E}_0 e^{ik_0 z}$ (where $k_0 = \omega/c$ and $\hat{\mathbf{e}}_z \cdot \mathbf{E}_0 = 0$) normally impinging upon a free-standing graphene ring on the $z = 0$ plane, whose inner and outer radii are a and b, respectively. The electromagnetic

response of the graphene ring (neglecting nonlocality and nonlinearity) can be modelled through the current density

$$\mathbf{J}(\mathbf{r}) = \sigma \mathbf{E}_{\perp}(\mathbf{r}_{\perp}) f(r_{\perp}) \delta(z), \tag{2}$$

where σ is the graphene surface conductivity at frequency ω, $\mathbf{r}_{\perp} = x\hat{\mathbf{e}}_x + y\hat{\mathbf{e}}_y$, $\mathbf{E}_{\perp}(\mathbf{r}_{\perp}) = E_x(\mathbf{r}_{\perp})\hat{\mathbf{e}}_x + E_y(\mathbf{r}_{\perp})\hat{\mathbf{e}}_y$ is the transverse component of the electric field on the ring and $f(r_{\perp})$ is the ring geometrical filling factor which is equal to zero if $r_{\perp} < a$ or $r_{\perp} > b$ and it is equal to one if $a + \delta < r_{\perp} < b - \delta$, where δ is a suitable edge layer thickness [6]. Due to the reduced dimensionality of the structure, the integral formalism is particularly suitable for describing radiation scattering. Since a time harmonic current density of complex amplitude $\mathbf{J}(\mathbf{r})$ radiates the field [7]

$$\mathbf{E}^{(\mathrm{s})}(\mathbf{r}) = \frac{i\omega\mu_0}{4\pi}\left(1 + \frac{1}{k_0^2}\nabla\nabla\cdot\right)\int d^3\mathbf{r}' \frac{e^{ik_0|\mathbf{r}-\mathbf{r}'|}}{|\mathbf{r}-\mathbf{r}'|}\mathbf{J}(\mathbf{r}'), \tag{3}$$

the overall electric field $\mathbf{E} = \mathbf{E}^{(\mathrm{i})} + \mathbf{E}^{(\mathrm{s})}$ in the presence of the graphene ring satisfies the equation

$$\mathbf{E}(\mathbf{r}) = \mathbf{E}_0 e^{ik_0 z} + \xi\frac{ik_0}{2\pi}\left(1 + \frac{1}{k_0^2}\nabla\nabla_{\perp}\cdot\right)\int d^2\mathbf{r}'_{\perp} \frac{e^{ik_0\sqrt{|\mathbf{r}_{\perp}-\mathbf{r}'_{\perp}|^2+z^2}}}{\sqrt{|\mathbf{r}_{\perp}-\mathbf{r}'_{\perp}|^2+z^2}} f(r'_{\perp})\mathbf{E}_{\perp}(\mathbf{r}'_{\perp}), \tag{4}$$

where $\xi = \frac{1}{2}\sqrt{\frac{\mu_0}{\varepsilon_0}}\sigma$ is the dimensionless graphene surface conductivity and $\nabla_{\perp} = \frac{\partial}{\partial x}\hat{\mathbf{e}}_x + \frac{\partial}{\partial y}\hat{\mathbf{e}}_y$. After evaluating the transverse part of Eq.(4) on the graphene ring (i.e. at $\mathbf{r} = \mathbf{r}_{\perp}$ with $a < r_{\perp} < b$) an integral equation for the electric field $\mathbf{E}_{\perp}(\mathbf{r}_{\perp})$ is obtained, and its solution allows the same Eq.(4) to provide the electric field over all the space. We are here only considering rings with size is much smaller than the radiation wavelength ($a < b \ll 2\pi/k_0$), and hence the integral equation reduces to its long-wavelength version

$$\mathbf{E}_{\perp}(\mathbf{r}_{\perp}) = \mathbf{E}_0 + \frac{i\xi}{2\pi k_0}\nabla_{\perp}\int d^2\mathbf{r}'_{\perp}\frac{\nabla'_{\perp}\cdot[f(r'_{\perp})\mathbf{E}_{\perp}(\mathbf{r}'_{\perp})]}{|\mathbf{r}_{\perp}-\mathbf{r}'_{\perp}|}, \tag{5}$$

where an integration by parts has been performed after noting that $\nabla_{\perp}|\mathbf{r}_{\perp}-\mathbf{r}'_{\perp}|^{-1} = -\nabla'_{\perp}|\mathbf{r}_{\perp}-\mathbf{r}'_{\perp}|^{-1}$. Such an approximation consists in neglecting retardation effects within the sub-wavelength structure and it entails an electrostatic description of the radiation-ring interaction. Physically, Eq.(5) states that the electric field produced by the ring on itself is due the effective surface charge density

$$\sigma_{\mathrm{sur}}(\mathbf{r}_{\perp}) = \frac{2\varepsilon_0\xi}{ik_0}\nabla_{\perp}\cdot[f(r_{\perp})\mathbf{E}_{\perp}(\mathbf{r}_{\perp})] \tag{6}$$

which self-consistently depends on the overall electric field. The electrostatic approximation allows one to introduce the electrostatic potential $V(\mathbf{r}_{\perp})$ for the electric field produced by the ring on itself according to

$$\mathbf{E}_{\perp}(\mathbf{r}_{\perp}) = \mathbf{E}_0 - \nabla_{\perp}V(\mathbf{r}_{\perp}) \tag{7}$$

so that Eq.(5) yields

$$V(\mathbf{r}_{\perp}) = V_0(\mathbf{r}_{\perp}) + \frac{i\xi}{2\pi k_0}\int d^2\mathbf{r}'_{\perp}\frac{\nabla'_{\perp}\cdot[f(r'_{\perp})\nabla'_{\perp}V(\mathbf{r}'_{\perp})]}{|\mathbf{r}_{\perp}-\mathbf{r}'_{\perp}|} \tag{8}$$

where

$$V_0(\mathbf{r}_{\perp}) = -\frac{i\xi}{2\pi k_0}\int d^2\mathbf{r}'_{\perp}\frac{\nabla'_{\perp}\cdot[f(r'_{\perp})\mathbf{E}_0]}{|\mathbf{r}_{\perp}-\mathbf{r}'_{\perp}|}. \tag{9}$$

Scattering of radiation with well-defined angular momentum. In this paper we are mainly focused on the impact of the field scattered by a subwavelength graphene ring on the rotational degrees of freedom of homonuclear molecules and therefore radiation with well-defined angular momentum would simplify and clarify such interaction at the same time. Since the graphene ring is rotationally invariant around the z axis, the z-component of the radiation angular momentum is conserved upon scattering. The generator of rotations around the z-axis (angular momentum) of any vector field is [8]

$$J_z = L_z + S_z, \tag{10}$$

where

$$L_z = \frac{1}{i}\left(x\frac{\partial}{\partial y} - y\frac{\partial}{\partial x}\right), \qquad S_z = \frac{1}{i}\begin{pmatrix} 0 & 1 & 0 \\ -1 & 0 & 0 \\ 0 & 0 & 0 \end{pmatrix}, \tag{11}$$

are the orbital and spin angular momentum operators, respectively. Hence, if the impinging field $\mathbf{E}^{(\mathrm{i})}$ is an eigenvector of J_z, the scattered field $\mathbf{E}^{(\mathrm{s})}$ is an eigenvector of J_z as well. In order to consider the simplest scattering situation compatible with rotational invariance, we here specialize the above general scattering approach to a circularly polarized impinging plane wave since it has a well-defined angular momentum and therefore we set

$$\mathbf{E}_0 = E_0\hat{\mathbf{e}}_{\mathrm{L}}, \tag{12}$$

where hereafter $\hat{\mathbf{e}}_{\mathrm{L}} = \frac{1}{\sqrt{2}}\left(\hat{\mathbf{e}}_x + i\hat{\mathbf{e}}_y\right)$ and $\hat{\mathbf{e}}_{\mathrm{R}} = \frac{1}{\sqrt{2}}\left(\hat{\mathbf{e}}_x - i\hat{\mathbf{e}}_y\right)$ are the left and right circular polarizations unit vectors, respectively. The angular momentum of such plane wave is of purely spin kind and it is equal to 1 (since $J_z\hat{\mathbf{e}}_{\mathrm{L}} = \hat{\mathbf{e}}_{\mathrm{L}}$) and hence the electric field $\mathbf{E} = \mathbf{E}^{(\mathrm{i})} + \mathbf{E}^{(\mathrm{s})}$ is an eigenvector of J_z with eigenvalue equal to 1 which is readily seen to have the general expression [9]

$$\mathbf{E}\left(r_\perp, \varphi, z\right) = \tilde{E}_{\mathrm{L}}\left(r_\perp, z\right)\hat{\mathbf{e}}_{\mathrm{L}} + \tilde{E}_{\mathrm{R}}\left(r_\perp, z\right)e^{i2\varphi}\hat{\mathbf{e}}_{\mathrm{R}} + \tilde{E}_z\left(r_\perp, z\right)e^{i\varphi}\hat{\mathbf{e}}_z, \tag{13}$$

where cylindrical coordinates have been introduced according to $x = r_\perp\cos\varphi$ and $y = r_\perp\sin\varphi$ and where hereafter the tilde is used for quantities independent on φ. Note that, even though the three components of the field in Eq.(13) are not independent, each of them is an eigenvector of J_z with eigenvalue 1 as it is simple to check after noting that the angular and spin angular momentum operators can be written as $L_z = \frac{1}{i}\frac{\partial}{\partial\varphi}$ and $S_z = \hat{\mathbf{e}}_{\mathrm{L}}\hat{\mathbf{e}}_{\mathrm{L}}^{\dagger} - \hat{\mathbf{e}}_{\mathrm{R}}\hat{\mathbf{e}}_{\mathrm{R}}^{\dagger}$, respectively. The emergence of the topological charges 2 and 1 (vortex generation) in the R- and z- components of the scattered field is required to compensate their spin angular momentum.

Since we are considering the circularly polarized components of the field by using cylindrical coordinates for the position, we report here the particularly useful expression of the nabla operator

$$\nabla = \frac{e^{-i\varphi}}{\sqrt{2}}\left(\frac{\partial}{\partial r_\perp} - \frac{i}{r_\perp}\frac{\partial}{\partial\varphi}\right)\hat{\mathbf{e}}_{\mathrm{L}} + \frac{e^{i\varphi}}{\sqrt{2}}\left(\frac{\partial}{\partial r_\perp} + \frac{i}{r_\perp}\frac{\partial}{\partial\varphi}\right)\hat{\mathbf{e}}_{\mathrm{R}} + \frac{\partial}{\partial z}\hat{\mathbf{e}}_z. \tag{14}$$

In addition, in order to clearly exploit the above discussed angular momentum conservation, it is also convenient to resort to the Bessel decomposition of the kernel of Eq.(4) [10]

$$\frac{1}{\sqrt{\left|\mathbf{r}_\perp - \mathbf{r}'_\perp\right|^2 + z^2}} = \int_0^{+\infty} dk_\perp e^{-k_\perp|z|}\sum_{n=-\infty}^{+\infty} J_n\left(k_\perp r_\perp\right)J_n\left(k_\perp r'_\perp\right)e^{in\left(\varphi-\varphi'\right)}. \tag{15}$$

Substituting Eq.(12) into Eq.(9), after using Eq.(14) and Eq.(15) with $z = 0$, we obtain after some algebra

$$V_0\left(\mathbf{r}_\perp\right) = -E_0\frac{i\xi}{k_0\sqrt{2}}\int_a^b dr'_\perp r'_\perp N\left(r_\perp, r'_\perp\right)\frac{df\left(r'_\perp\right)}{dr'_\perp}e^{i\varphi} \equiv \tilde{V}_0\left(r_\perp\right)e^{i\varphi} \tag{16}$$

where $N\left(r_\perp, r'_\perp\right) = \int_0^{+\infty} dk_\perp J_1\left(k_\perp r_\perp\right)J_1\left(k_\perp r'_\perp\right)$ and we have used the fact that $df/dr_\perp$ vanishes for $r_\perp < a$ and $r_\perp > b$. The integral in the kernel $N\left(r_\perp, r'_\perp\right)$ can be analytically performed [11] so that we obtain

$$N\left(r_\perp, r'_\perp\right) = \frac{r_\perp r'_\perp}{2\left(r_\perp + r'_\perp\right)^3}\,{}_2F_1\left(\frac{3}{2}, \frac{3}{2}; 3; \frac{4r_\perp r'_\perp}{\left(r_\perp + r'_\perp\right)^2}\right) \tag{17}$$

where ${}_2F_1\left(a, b; c; \xi\right)$ is the hypergeometric function. Equation (16) states that the left circular polarization of the impinging field imposes a topological charge 1 to the source term of Eq.(8) and this implies that the potential also has the same property, i.e.

$$V\left(\mathbf{r}_\perp\right) = \tilde{V}\left(r_\perp\right)e^{i\varphi}. \tag{18}$$

This is due to the fact that, after substituting Eq.(18) into Eq.(8) and using Eqs.(16), (15) and (14), we obtain

$$\tilde{V}(r_\perp) = \tilde{V}_0(r_\perp) + \frac{i\xi}{k_0}\int_a^b dr'_\perp r'_\perp N(r_\perp, r'_\perp)\left[f(r'_\perp)\left(\frac{d^2}{dr'^2_\perp} + \frac{1}{r'_\perp}\frac{d}{dr'_\perp} - \frac{1}{r'^2_\perp}\right) + \frac{df(r'_\perp)}{dr'_\perp}\frac{d}{dr'_\perp}\right]\tilde{V}(r'_\perp) \tag{19}$$

which is a one-dimensional integral equation for the radial part $\tilde{V}(r_\perp)$ of the potential. In other words conservation of angular momentum upon scattering implies that the potential on the ring has a definite topological charge equal to the value of the impinging angular momentum.

Once $\tilde{V}(r_\perp)$ is obtained by solving Eq.(19), Eq.(7) provides the transverse electric field on the graphene ring which, using Eq.(14), becomes

$$\mathbf{E}_\perp(\mathbf{r}_\perp) = \left[E_0 - \frac{1}{\sqrt{2}}\left(\frac{d}{dr_\perp} + \frac{1}{r_\perp}\right)\tilde{V}(r_\perp)\right]\hat{\mathbf{e}}_\mathrm{L} + \left[-\frac{1}{\sqrt{2}}\left(\frac{d}{dr_\perp} - \frac{1}{r_\perp}\right)\tilde{V}(r_\perp)e^{i2\varphi}\right]\hat{\mathbf{e}}_\mathrm{R} \tag{20}$$

whose structure evidently agrees with angular momentum conservation (see Eq.(13)). Substituting Eq.(20) into Eq.(6) and using again Eq.(14) we get

$$\sigma_\mathrm{sur}(\mathbf{r}_\perp) = \frac{2\varepsilon_0\xi}{ik_0}\left\{\frac{df(r_\perp)}{dr_\perp}\frac{E_0}{\sqrt{2}} - \left[f(r_\perp)\left(\frac{d^2}{dr_\perp^2} + \frac{1}{r_\perp}\frac{d}{dr_\perp} - \frac{1}{r_\perp^2}\right) + \frac{df(r_\perp)}{dr_\perp}\frac{d}{dr_\perp}\right]\tilde{V}(r_\perp)\right\}e^{i\varphi} \equiv \tilde{\sigma}_\mathrm{sur}(r_\perp)e^{i\varphi} \tag{21}$$

so that the surface charge density has topological charge 1 as well, as expected since it is the source of the potential.

The integral equation provided by Eq.(19) can not be analytically dealt with. However, after noting that the integral in Eq.(15) can be analytically evaluated and written in terms of hypergeometric functions, Eq.(19) can be approximated by a matrix equation by writing the potential as

$$\tilde{V}(r_\perp) = \sum_{n=0}^{N} c_n \Psi_n(r_\perp), \tag{22}$$

where the function $\Psi_n(r_\perp)$ are a suitable orthonormal basis on the interval $[a, b]$. In our numerical analysis we have chosen the basis functions

$$\Psi_n(r_\perp) = \sqrt{\frac{2n+1}{b-a}}P_n\left(\frac{2r_\perp - b - a}{b-a}\right), \tag{23}$$

where $P_n(z)$ is the n-th Legendre polynomial, which are easily seen to satisfy the orthonormality relation

$$\int_a^b dr_\perp \Psi_n(r_\perp)\Psi_m(r_\perp) = \delta_{nm}. \tag{24}$$

In all numerical calculations we have checked that excellent convergence is achieved by using only the first $N = 25$ basis functions.

Resonant scattering. In the present analysis, we are proving that the field scattered by the graphene ring can trigger a highly nontrivial radiation-matter interaction regime where the standard multipole treatment is challenged. To achieve this goal, the interacting field should not be regarded as uniform on the molecule spatial scale so that it should have deep sub-wavelength spatial features. A field with such spatial properties can be achieved by resorting to the resonant scattering provided by the graphene ring together with a suitable tailoring of the ring size. To discuss this point, note that Eq.(19) can be written as

$$\tilde{V} = \tilde{V}_0 + i\xi K\tilde{V} \tag{25}$$

where K is the integral operator

$$\left[K\tilde{V}\right](r_\perp) = \frac{1}{k_0}\int_a^b dr'_\perp r'_\perp N(r_\perp, r'_\perp)\left[f(r'_\perp)\left(\frac{d^2}{dr'^2_\perp} + \frac{1}{r'_\perp}\frac{d}{dr'_\perp} - \frac{1}{r'^2_\perp}\right) + \frac{df(r'_\perp)}{dr'_\perp}\frac{d}{dr'_\perp}\right]\tilde{V}(r'_\perp). \tag{26}$$

Assuming that the operator K admits a complete (even not orthonormal) set of modal eigenvectors

$$K\tilde{\varphi}_n = \kappa_n\tilde{\varphi}_n \tag{27}$$

the solution of Eq.(25) is readily seen to be

$$\tilde{V}\left(r_{\perp}\right)=\sum_{n}\frac{c_{n}}{1-i\xi\kappa_{n}}\tilde{\varphi}_{n}\left(r_{\perp}\right) \tag{28}$$

where c_n are the coefficients in the expansion $\tilde{V}_0\left(r_{\perp}\right)=\sum\limits_{n}c_{n}\tilde{\varphi}_{n}\left(r_{\perp}\right)$. Evidently, if the field frequency and the graphene doping are such that $\xi\simeq-\frac{i}{\kappa_m}$ for a specific m, the term with $n=m$ will dominate the series of Eq.(28), i.e. the excitation is resonant with the $m-$th ring mode. Accordingly the surface-charge density $\tilde{\sigma}_{\mathrm{sur}}(r_{\perp})$ in Eq.(21) becomes very large especially close to ring edges with a corresponding local very large field enhancement. In order to achieve a scattered field with very deep-subwavelength spatial feature it is therefore sufficient to choose the inner ring radius a to be very much smaller than the wavelength as detailed in the main manuscript.

In order to characterize the efficiency of a scattering experiment, it is convenient to obtain the absorption cross section of the process. The dipole moment of the ring

$$\mathbf{p}=\int d^{2}\mathbf{r}_{\perp}\mathbf{r}_{\perp}\sigma_{\mathrm{sur}}\left(\mathbf{r}_{\perp}\right), \tag{29}$$

after using Eq.(21) and the relation $\mathbf{r}_{\perp}=\frac{r_{\perp}}{\sqrt{2}}\left(e^{-i\varphi}\hat{\mathbf{e}}_{\mathrm{L}}+e^{i\varphi}\hat{\mathbf{e}}_{\mathrm{R}}\right)$, can be written as

$$\mathbf{p}=\left[\frac{\sqrt{2}\pi}{E_{0}}\int\limits_{a}^{b}dr_{\perp}r_{\perp}^{2}\tilde{\sigma}_{\mathrm{sur}}\left(r_{\perp}\right)\right]\mathbf{E}_{0}\equiv\alpha\mathbf{E}_{0} \tag{30}$$

so that the polarizability α can be simply evaluated from the radial part of the surface charge density. From the optical theorem and the far-field structure of the dipole radiation [7], the expression for the absorption cross section $\sigma_{\mathrm{abs}}=\frac{k_0}{\varepsilon_0}\mathrm{Im}\alpha$ is easily obtained, so that we get

$$\sigma_{\mathrm{abs}}=\frac{\sqrt{2}\pi k_{0}}{\varepsilon_{0}E_{0}}\mathrm{Im}\int\limits_{a}^{b}dr_{\perp}r_{\perp}^{2}\tilde{\sigma}_{\mathrm{sur}}\left(r_{\perp}\right). \tag{31}$$

Deep-subwavelength spatial features of the scattered near field. The interaction of the field scattered by the graphene ring and homonuclear molecules is expected to be highly nontrivial on the region surrounding the ring where the field gradient is very pronounced. Therefore we focus on the near-field ($r\ll2\pi/k_0=\lambda$) approximating Eq.(4) in the form

$$\mathbf{E}\left(\mathbf{r}\right)=\mathbf{E}_{0}e^{ik_{0}z}-\nabla\left[\frac{1}{4\pi\varepsilon_{0}}\int d^{2}\mathbf{r}_{\perp}^{\prime}\frac{\sigma_{\mathrm{sur}}\left(\mathbf{r}_{\perp}^{\prime}\right)}{\sqrt{\left|\mathbf{r}_{\perp}-\mathbf{r}_{\perp}^{\prime}\right|^{2}+z^{2}}}\right], \tag{32}$$

where Eq.(6) has been used to replace the divergence with the surface charge densities. Using Eq.(15), Eq.(14) and some well-known properties of the Bessel functions, it is easy to show that the electric field has the structure of Eq.(13) where

$$\begin{aligned}
\tilde{E}_{\mathrm{L}}\left(r_{\perp},z\right) &= E_{0}e^{ik_{0}z}-\frac{1}{2\sqrt{2}\varepsilon_{0}}\int\limits_{a}^{b}dr_{\perp}^{\prime}r_{\perp}^{\prime}N_{0}\left(r_{\perp},r_{\perp}^{\prime};z\right)\tilde{\sigma}_{\mathrm{sur}}\left(r_{\perp}^{\prime}\right),\\
\tilde{E}_{\mathrm{R}}\left(r_{\perp},z\right) &= \frac{1}{2\sqrt{2}\varepsilon_{0}}\int\limits_{a}^{b}dr_{\perp}^{\prime}r_{\perp}^{\prime}N_{2}\left(r_{\perp},r_{\perp}^{\prime};z\right)\tilde{\sigma}_{\mathrm{sur}}\left(r_{\perp}^{\prime}\right),\\
\tilde{E}_{z}\left(r_{\perp},z\right) &= \frac{\mathrm{sign}\left(z\right)}{2\varepsilon_{0}}\int\limits_{a}^{b}dr_{\perp}^{\prime}r_{\perp}^{\prime}N_{1}\left(r_{\perp},r_{\perp}^{\prime};z\right)\tilde{\sigma}_{\mathrm{sur}}\left(r_{\perp}^{\prime}\right),
\end{aligned} \tag{33}$$

where

$$N_{n}\left(r_{\perp},r_{\perp}^{\prime};z\right)=\int\limits_{0}^{+\infty}dk_{\perp}k_{\perp}e^{-k_{\perp}|z|}J_{n}\left(k_{\perp}r_{\perp}\right)J_{1}\left(k_{\perp}r_{\perp}^{\prime}\right). \tag{34}$$

In addition to revealing that the electric field has the structure imposed by the conservation of angular momentum even in the near-field, Eqs.(33) are particularly suitable for evaluation purposes since the integrals in the kernels $N_n\left(r_\perp, r'_\perp; z\right)$ can be analytically evaluated [11] and we obtain

$$\begin{aligned} N_0\left(r_\perp, r'_\perp; z\right) &= \frac{m}{8\pi\left(1-m^2\right)}\left[\frac{m^2\left(-r_\perp^2+r_\perp'^2-z^2\right)E\left(m\right)+4r_\perp r'_\perp\left(1-m^2\right)K\left(m\right)}{r_\perp^{3/2}r_\perp'^{5/2}}\right], \\ N_2\left(r_\perp, r'_\perp; z\right) &= -N_0\left(r_\perp, r'_\perp; z\right)+\frac{2}{\pi m}\left[\frac{\left(2-m^2\right)K\left(m\right)-2E\left(m\right)}{r_\perp^{3/2}r_\perp'^{1/2}}\right], \\ N_1\left(r_\perp, r'_\perp; z\right) &= \frac{m}{4\pi\left(1-m^2\right)}\left|z\right|\left[\frac{\left(2-m^2\right)E\left(m\right)-2\left(1-m^2\right)K\left(m\right)}{r_\perp^{3/2}r_\perp'^{3/2}}\right]. \end{aligned} \tag{35}$$

where $K\left(m\right)=\int\limits_0^{\pi/2}d\tau\left(1-m^2\sin^2\tau\right)^{-1/2}$ and $E\left(m\right)=\int\limits_0^{\pi/2}d\tau\left(1-m^2\sin^2\tau\right)^{1/2}$ are the complete elliptic integrals of the first and second kind, respectively, and

$$m=\sqrt{\frac{4r_\perp r'_\perp}{\left(r_\perp+r'_\perp\right)^2+z^2}}. \tag{36}$$

It is worth discussing the behavior of the field close to the inner edge of the ring (at $r_\perp=a$). Our numerical analysis of the scattering process reveals that the surface-charge density $\tilde{\sigma}_{\rm sur}\left(r_\perp\right)$ attains very large values only close to the ring edges $r_\perp=a$ and $r_\perp=b$ (especially at resonance where we are mainly investigating radiation-matter interaction). Due to the nano-size of the ring hole, the contribution of $\tilde{\sigma}_{\rm sur}(a)$ close to $r_\perp=a$ is expected to be dominant for points close to the inner edge of the ring. As a consequence, for $r_\perp<a$ and $|z|<a$, an estimation of the integrals in Eqs.(33) can obtained by restricting the integration to a very small domain $a<r'_\perp<a(1+\eta)$ (with $\eta<<1$) and by assuming $\tilde{\sigma}_{\rm sur}$ to be constant over such domain. For simplicity, we focus on the left-hand circular component of the field whose estimation yields

$$\tilde{E}_{\rm L}\left(r_\perp, z\right)=E_0e^{ik_0z}-\frac{\tilde{\sigma}_{\rm sur}\left(a\right)}{\varepsilon_0}\frac{\eta}{2\sqrt{2}}F\left(\frac{r_\perp}{a},\frac{z}{a}\right) \tag{37}$$

where, from the first of Eqs.(35), we have

$$F\left(\rho,\zeta\right)=\frac{1}{\pi\sqrt{\left(\rho+1\right)^2+\zeta^2}}\left[\left(\frac{1-\rho^2-\zeta^2}{\left(\rho-1\right)^2+\zeta^2}\right)E\left(\sqrt{\frac{4\rho}{\left(\rho+1\right)^2+\zeta^2}}\right)+K\left(\sqrt{\frac{4\rho}{\left(\rho+1\right)^2+\zeta^2}}\right)\right] \tag{38}$$

Even if such estimation is rather crude, it sheds light on a number of relevant features characterizing the actual field scattered by the graphene ring. In first place Eq.(37) clearlys show that the resonant scattering is accompanied by a large field enhancement since numerical analysis reveals that $\frac{|\tilde{\sigma}_{\rm sur}(a)|}{\varepsilon_0}\gg E_0$. Second, Eq.(38) shows that at the graphene ring plane $\zeta=0$ the function $F\left(\rho,0\right)$ diverges for $\rho\to1$ thus clearly stating that the actual scattered field close inside to the inner ring edge is extremely larger that at the center of the ring. Since in the present analysis we have chosen a to be very much smaller than the wavelength (which has been set in the Terahertz domain in the main paper), it is evident that the scattered field is characterized by an extremely deep sub-wavelength scale inside the ball $r<a$. Such spatial feature is precisely the ingredient able to trigger a highly nontrivial radiation-matter interaction in principle not treatable in terms of the standard multipole expansion. To discuss this point, in Supplementary Fig.1 we have plotted the function $F\left(\rho,\zeta\right)$ for $0.9<\rho<1$ at the planes $\zeta=1,2,3,4,5\cdot10^{-4}$ and, in the inset, we have highlighted that for $0.985<\rho<0.995$ the function $F\left(\rho,10^{-4}\right)$ displays a large variation which can not be linearized. If we set $a=15$ nm (as done in the main text), such region has a width of about 1.5 Å which is of the order of the molecule size (see below) and this implies that, when describing radiation matter interaction, it is generally not possible to retain only the slowest order of the field expansion around the center of the mass of the molecule.

Spherical harmonic expansion of the field inside the ring hole. A different (but equivalent) way of investigating the very fast spatial scale of the scattered field is provided by the radial Taylor expansion of the field around the center of the ring. In order to achieve this goal, we exploit the relation [7]

$$\frac{1}{|\mathbf{r}-\mathbf{r}'|}=4\pi\sum_{l=0}^{\infty}\sum_{m=-l}^{l}\frac{1}{2l+1}\frac{r_<^l}{r_>^{l+1}}Y_l^{m*}\left(\theta',\varphi'\right)Y_l^m\left(\theta,\varphi\right) \tag{39}$$

where spherical coordinates have been introduced ($x = r\sin\theta\cos\varphi$, $y = r\sin\theta\sin\varphi$, $z = r\cos\theta$), $r_>$ and $r_<$ are the larger and the smaller of r and r', respectively and $Y_l^m(\theta,\varphi)$ are the spherical harmonics. In view of Eq.(32), we note that $\mathbf{r}' = \mathbf{r}'_\perp$ and $\theta' = \frac{\pi}{2}$ and that $r < r'$ on the sphere $r < a$ embedded within ring hole so that Eq.(39) becomes

$$\frac{1}{\sqrt{|\mathbf{r}_\perp - \mathbf{r}'_\perp|^2 + z^2}} = 4\pi \sum_{l=0}^{\infty}\sum_{m=-l}^{l} \frac{1}{2l+1}\frac{r^l}{(r'_\perp)^{l+1}} Y_l^{m*}\left(\frac{\pi}{2},\varphi'\right) Y_l^m(\theta,\varphi). \tag{40}$$

Inserting Eq.(40) into Eq.(32), using Eq.(21) together with the familiar expression for the spherical harmonics $Y_l^m(\theta,\varphi) = \sqrt{\frac{2l+1}{4\pi}\frac{(l-m)!}{(l+m)!}}P_l^m(\cos\theta)\,e^{im\varphi}$ and performing the trivial integration over φ', we get for the scattered field $\mathbf{E}^{(\mathrm{s})}(\mathbf{r}) = \mathbf{E}(\mathbf{r}) - \mathbf{E}_0 e^{ik_0 z}$ within the sphere $r < a$

$$\mathbf{E}^{(\mathrm{s})}(\mathbf{r}) = -\nabla \sum_{l=0}^{\infty}\left[\frac{1}{\varepsilon_0}\int_a^b dr'_\perp \frac{\tilde{\sigma}_{\mathrm{sur}}(r'_\perp)}{(r'_\perp)^l}\right]\sqrt{\frac{\pi}{(2l+1)}\frac{(l-1)!}{(l+1)!}}P_l^1(0) r^l Y_l^1(\theta,\varphi). \tag{41}$$

The associated Legendre functions have the property

$$P_l^1(0) = \begin{cases} (-1)^{(l+1)/2}\dfrac{l!!}{(l-1)!!}, & \text{if } l \text{ odd},\\ 0, & \text{if } l \text{ even}, \end{cases} \tag{42}$$

so that Eq.(41) turns into

$$\mathbf{E}^{(s)}(\mathbf{r}) = \sum_{s=0}^{\infty}\left[\frac{1}{\varepsilon_0}\int_1^{b/a} d\rho \frac{\tilde{\sigma}_{\mathrm{sur}}(a\rho)}{\rho^{2s+1}}\right]\left[(-1)^s\frac{(2s+1)!!}{(2s)!!}\sqrt{\frac{\pi}{(4s+3)}\frac{(2s)!}{(2s+2)!}}\right]\frac{1}{a^{2s}}\nabla\left[r^{2s+1}Y_{2s+1}^1(\theta,\varphi)\right], \tag{43}$$

where we have set $r'_\perp = a\rho$ to get a dimensionless integral. Note that the potential of the scattered field is the superposition of only the spherical harmonics Y_l^m of order $m = 1$, as it was expected from conservation of angular momentum, and of odd degree $l = 2s+1$ since such potential is spatially odd as a consequence of the topological charge 1 of the surface charge density. The gradient of the harmonic polynomial $r^l Y_l^m(\theta,\varphi)$ can be evaluated by using the expression of the nabla operator

$$\begin{aligned}\nabla \;=\; & \frac{e^{-i\varphi}}{\sqrt{2}}\left[\sin\theta\frac{\partial}{\partial r} + \frac{1}{r}\left(\cos\theta\frac{\partial}{\partial\theta} - \frac{i}{\sin\theta}\frac{\partial}{\partial\varphi}\right)\right]\hat{\mathbf{e}}_{\mathrm{L}} + \frac{e^{i\varphi}}{\sqrt{2}}\left[\sin\theta\frac{\partial}{\partial r} + \frac{1}{r}\left(\cos\theta\frac{\partial}{\partial\theta} + \frac{i}{\sin\theta}\frac{\partial}{\partial\varphi}\right)\right]\hat{\mathbf{e}}_{\mathrm{R}} + \\ & + \left(\cos\theta\frac{\partial}{\partial r} - \frac{\sin\theta}{r}\frac{\partial}{\partial\theta}\right)\hat{\mathbf{e}}_z.\end{aligned} \tag{44}$$

so that, after some algebra, we obtain

$$\begin{aligned}\nabla\left[r^l Y_l^1(\theta,\varphi)\right] \;=\; & r^{l-1}\sqrt{\frac{2l+1}{2l-1}}\left\{\left[-\sqrt{\frac{l(l+1)}{2}}Y_{l-1}^0(\theta,\varphi)\right]\hat{\mathbf{e}}_{\mathrm{L}} + \left[\sqrt{\frac{(l-1)(l-2)}{2}}Y_{l-1}^2(\theta,\varphi)\right]\hat{\mathbf{e}}_{\mathrm{R}}\right\} + \\ & + r^{l-1}\sqrt{\frac{2l+1}{2l-1}}\left[\sqrt{(l+1)(l-1)}Y_{l-1}^1(\theta,\varphi)\right]\hat{\mathbf{e}}_z,\end{aligned} \tag{45}$$

where the well-known properties of the associated Legendre functions

$$\begin{aligned}\frac{\partial P_l^m(\xi)}{\partial\xi} \;&=\; \frac{1}{\xi^2-1}\left[\xi l P_l^m(\xi) - (m+l)P_{l-1}^m(\xi)\right],\\ P_l^{m-1}(\xi) \;&=\; \frac{\xi P_l^m(\xi) - P_{l+1}^m(\xi)}{(l+m)\sqrt{1-\xi^2}},\\ P_l^{m+1}(\xi) \;&=\; \frac{(l-m+1)P_{l+1}^m(\xi) - (l+m+1)\xi P_l^m(\xi)}{\sqrt{1-\xi^2}}\end{aligned} \tag{46}$$

have been used. Using Eq.(45), Eq.(43) yields

$$\mathbf{E}^{(\mathrm{s})}(r,\theta,\varphi) = \sum_{s=0}^{\infty} F_s\left[\frac{C_s^0}{\sqrt{2}}Y_{2s}^0(\theta,\varphi)\hat{\mathbf{e}}_{\mathrm{L}} + \frac{C_s^2}{\sqrt{2}}Y_{2s}^2(\theta,\varphi)\hat{\mathbf{e}}_{\mathrm{R}} + C_s^1 Y_{2s}^1(\theta,\varphi)\hat{\mathbf{e}}_z\right]\left(\frac{r}{a}\right)^{2s}, \tag{47}$$

where

$$
\begin{aligned}
F_s &= \frac{1}{\varepsilon_0}\int_1^{b/a} d\rho \frac{\tilde{\sigma}_{\rm sur}\left(a\rho\right)}{\rho^{2s+1}},\\
C_s^0 &= (-1)^{s+1}\frac{(2s+1)!!}{(2s)!!}\sqrt{\frac{\pi}{(4s+1)}},\\
C_s^2 &= (-1)^{s}\frac{(2s+1)!!}{(2s)!!}\sqrt{\frac{\pi}{(4s+1)}\frac{s\left(2s-1\right)}{(s+1)\left(2s+1\right)}},\\
C_s^1 &= (-1)^{s}\frac{(2s+1)!!}{(2s)!!}\sqrt{\frac{\pi}{(4s+1)}\frac{2s}{(2s+1)}}.
\end{aligned}
\tag{48}
$$

Equation (47) provides the full expansion of the scattered electric field on the sphere $r < a$. The three field components are the superposition of only the spherical harmonic $Y_l^m(\theta,\varphi)$ with even degree $l = 2s$ (since the field is spatially even) and with a single order, i.e. $m = 0$, $m = 2$ and $m = 1$ for the left, right and $z-$ components, respectively. Once again this is in agreement with the general structure of a field with angular momentum equal to 1 (see Eq.(13)) since, $r_\perp = r\cos\theta$, $z = r\sin\theta$, $Y_l^m(\theta,\varphi) = f_l^m(\theta)e^{im\varphi}$ and cylindrical and spherical coordinates have the same azimuthal angle φ. The coefficients C_s^m are purely geometrical and it is simple to show that

$$
\begin{aligned}
|C_s^m| &< 1,\\
\lim_{s\to\infty}|C_s^m| &= 1,
\end{aligned}
\tag{49}
$$

this implying that the rate of convergence of the series is only due to the terms F_s. On the other hand, the surface-charge density $\tilde{\sigma}_{\rm sur}$ attains very large values only close to the inner ring edge $r_\perp = a$. As a consequence, the first of Eqs.(48) can be approximated by restricting the integration to a very small domain $1 < \rho < 1+\eta$ (with $\eta << 1$) and by assuming $\tilde{\sigma}_{\rm sur}$ to be constant over such domain, thus obtaining

$$
F_s \simeq \frac{\tilde{\sigma}_{\rm sur}\left(a\right)}{\varepsilon_0}\int_1^{1+\eta} d\rho\,\frac{1}{\rho^{2s+1}} = \frac{\tilde{\sigma}_{\rm sur}\left(a\right)}{\varepsilon_0}\frac{1}{2s}\left[1-\frac{1}{\left(1+\eta\right)^{2s}}\right] \simeq \frac{\tilde{\sigma}_{\rm sur}\left(a\right)}{\varepsilon_0}\left[\eta-\left(s+\frac{1}{2}\right)\eta^2\right],
\tag{50}
$$

which reveals that the coefficients F_s are very slowly dependent on s, the first order in η being independent on s at all. This implies that the expansion of Eq.(47) is very slowly convergent in the parameter r/a so that the scattered field displays a very pronounced variation for $0 < r < a$. An equivalent way to prove this statement is noting that, due to above properties of the coefficients F_s and C_s^m, the components of scattered field of Eq.(47) can mainly be modelled, if the spherical harmonics are neglected, by the function

$$
\sum_{s=0}^{\infty}\left(\frac{r}{a}\right)^{2s} = \frac{a^2}{a^2-r^2}
\tag{51}
$$

whose divergence at $r = a$ clearly shows that the actual scattered field close inside to the inner ring edge is extremely larger that at the center of the ring. Since in the present analysis we have chosen a to be very much smaller than the wavelength, it is evident that the scattered field is characterized by an extremely deep sub-wavelength scale inside the ball $r < a$.

Supplementary Note 2

Rotational transitions. In order to investigate the interaction of matter with the field scattered by the graphene ring, as a case study, we here consider the hydrogen molecular ion (H_2^+) which is the simplest molecule in nature. The molecule is composed of two protons at the positions $r_{\rm A}$ and $r_{\rm B}$ and an electron at $r_{\rm e}$. After introducing the standard center of the mass and relative coordinates

$$
\begin{aligned}
\mathbf{R}_{\rm c} &= \frac{1}{2}\left(\mathbf{R}_{\rm A}+\mathbf{R}_{\rm B}\right),\\
\mathbf{R} &= \mathbf{R}_{\rm B}-\mathbf{R}_{\rm A},\\
\mathbf{r} &= \mathbf{r}_{\rm e}-\frac{1}{2}\left(\mathbf{R}_{\rm A}+\mathbf{R}_{\rm B}\right),
\end{aligned}
\tag{52}
$$

in the Born-Oppenheimer approximation [12], the molecule eigenfunctions Ψ (such that $\hat{H}\Psi = E\Psi$) have the familiar factorization

$$\Psi\left(\mathbf{R}_{\mathrm{c}}, \mathbf{R}, \mathbf{r}\right) = \Psi^{(\mathrm{c})}\left(\mathbf{R}_{\mathrm{c}}\right) \Psi^{(\mathrm{e})}\left(\mathbf{R}, \mathbf{r}\right) \Psi^{(\mathrm{N})}\left(\mathbf{R}\right) \tag{53}$$

where the center of the mass $\Psi^{(\mathrm{c})}$, electronic $\Psi^{(\mathrm{e})}$ and nuclear $\Psi^{(\mathrm{N})}$ wave functions satisfy the Schrödinger equations

$$\begin{aligned}
\left[-\frac{\hbar^2}{4M}\nabla^2_{\mathbf{R}_{\mathrm{c}}}\right] \Psi^{(\mathrm{c})}\left(\mathbf{R}_{\mathrm{c}}\right) &= E^{(\mathrm{c})}\Psi^{(\mathrm{c})}\left(\mathbf{R}_{\mathrm{c}}\right), \\
\left[-\frac{\hbar^2}{2m}\nabla^2_{\mathbf{r}} + \frac{e^2}{4\pi\varepsilon_0}\left(\frac{1}{\mathbf{R}} - \frac{1}{|\mathbf{r}+\mathbf{R}/2|} - \frac{1}{|\mathbf{r}-\mathbf{R}/2|}\right)\right] \Psi^{(\mathrm{e})}\left(\mathbf{R}, \mathbf{r}\right) &= E^{(\mathrm{e})}\left(R\right) \Psi^{(\mathrm{e})}\left(\mathbf{R}, \mathbf{r}\right), \\
\left[-\frac{\hbar^2}{M}\nabla^2_{\mathbf{R}} + E^{(e)}\left(\mathbf{R}\right)\right] \Psi^{(\mathrm{N})}\left(\mathbf{R}\right) &= E^{(\mathrm{N})}\Psi^{(\mathrm{N})}\left(\mathbf{R}\right),
\end{aligned} \tag{54}$$

where m and M are the electron and proton mass, respectively and the energy eigenvalue is $E = E^{(\mathrm{c})} + E^{(\mathrm{N})}$. In the discussion below, we will be mainly concerned with rotational transitions and hence we will only consider the electronic ground state $\Psi^{(e)}\left(\mathbf{R}, \mathbf{r}\right)$. Neglecting centrifugal distortion, the nuclear eigenfunctions associated to the electronic ground state are

$$\Psi^{(\mathrm{N})}_{n,J,M}\left(\mathbf{R}\right) = \frac{1}{R} G_n\left(R\right) Y^M_J\left(\Theta, \Phi\right), \tag{55}$$

where (R, Θ, Φ) are the spherical coordinates of the internuclear vector $\mathbf{R}$, $Y^M_J\left(\Theta, \Phi\right)$ are the spherical harmonics, (n, J, M) are the vibrational, rotational and magnetic quantum numbers, respectively, and

$$G_n\left(R\right) = \left(\frac{M\omega_{\mathrm{e}}}{2\pi\hbar}\right)^{1/4} \frac{1}{\sqrt{2^n n!}} e^{-\frac{M\omega_{\mathrm{e}}}{4\hbar}\left(R-R_{\mathrm{e}}\right)^2} H_n\left[\left(\frac{M\omega_{\mathrm{e}}}{2\hbar}\right)^{1/2}\left(R - R_{\mathrm{e}}\right)\right], \tag{56}$$

where $R_{\mathrm{e}} = 1.06$ Å is the internuclear equilibrium distance, $\omega_{\mathrm{e}} = \left(\frac{2}{M}\left.\frac{d^2E^{(\mathrm{e})}}{dR^2}\right|_{\mathrm{R}_e}\right)^{1/2}$ is the fundamental vibrational angular frequency ($\bar{\nu}_{\mathrm{e}} = \frac{\omega_{\mathrm{e}}}{2\pi c} = 2297$ cm^{-1}) and $H_n(\xi)$ is the $n-$th Hermite polynomial [12]. The energy eigenvalue of the eigenfunction $\Psi^{(\mathrm{N})}_{n,J,M}\left(\mathbf{R}\right)$ is

$$E^{(\mathrm{N})}_{n,J} = E^{(\mathrm{e})}\left(R_{\mathrm{e}}\right) + \hbar\omega_{\mathrm{e}}\left(n + \frac{1}{2}\right) + BJ\left(J+1\right), \tag{57}$$

where $B = \frac{\hbar^2}{MR^2_{\mathrm{e}}}$ is the fundamental rotational constant ($\bar{B} = \frac{2\pi}{\hbar c}B = 29.8$ cm^{-1}).

We investigate the molecule-radiation interaction by resorting to the Power-Zienau-Woolley [13] scheme according to which the interaction hamiltonian is

$$H_{\mathrm{I}} = -\int d^3\mathbf{r}\, \mathbf{P}\left(\mathbf{r}\right) \cdot \mathsf{E}\left(\mathbf{r}, t\right), \tag{58}$$

where $\mathsf{E}\left(\mathbf{r}, t\right) = \mathrm{Re}\left[\mathbf{E}\left(\mathbf{r}\right) e^{-i\omega t}\right]$ is the real electric field and $\mathbf{P}\left(\mathbf{r}\right)$ is the polarization density which, for a system of point charges (of charge q_α and located at $\mathbf{r}_\alpha$) localized around the point $\bar{\mathbf{R}}$, is

$$\mathbf{P}\left(\mathbf{r}\right) = \sum_\alpha q_\alpha\left(\mathbf{r}_\alpha - \bar{\mathbf{R}}\right) \int_0^1 du\, \delta\left[\mathbf{r} - \bar{\mathbf{R}} - u\left(\mathbf{r}_\alpha - \bar{\mathbf{R}}\right)\right]. \tag{59}$$

Since in the present analysis we only focus on absorption spettroscopy, in Eq.(58) we can retained only the positive frequency part of the electric field $\frac{1}{2}\mathbf{E}\left(\mathbf{r}\right)$ (also dropping the time dependent term $e^{-i\omega t}$). For the hydrogen molecular ion we have $q_1 = -e$, $q_2 = e$, $q_3 = e$ and $\mathbf{r}_1 = \mathbf{r}_e$, $\mathbf{r}_2 = \mathbf{R}_{\mathrm{A}}$, $\mathbf{r}_3 = \mathbf{R}_{\mathrm{B}}$ so that, after choosing $\bar{\mathbf{R}} = \mathbf{R}_{\mathrm{c}}$, inserting Eq.(59) into Eq.(58) and using Eqs.(52), we get

$$H_{\mathrm{I}}\left(\mathbf{R}_{\mathrm{c}}, \mathbf{R}, \mathbf{r}\right) = H^{(\mathrm{e})}_{\mathrm{I}}\left(\mathbf{R}_{\mathrm{c}}, \mathbf{r}\right) + H^{(\mathrm{N})}_{\mathrm{I}}\left(\mathbf{R}_{\mathrm{c}}, \mathbf{R}\right), \tag{60}$$

where

$$H_{\rm I}^{(\rm e)}\left(\mathbf{R}_{\rm c},\mathbf{r}\right) = \frac{e}{2}\mathbf{r}\cdot\int_0^1 du\,\mathbf{E}\left(\mathbf{R}_{\rm c}+u\mathbf{r}\right),$$
$$H_{\rm I}^{(\rm N)}\left(\mathbf{R}_{\rm c},\mathbf{R}\right) = \frac{e}{4}\mathbf{R}\cdot\int_0^1 du\left[\mathbf{E}\left(\mathbf{R}_{\rm c}-u\frac{\mathbf{R}}{2}\right)-\mathbf{E}\left(\mathbf{R}_{\rm c}+u\frac{\mathbf{R}}{2}\right)\right] \quad (61)$$

are the electronic and nuclear contributions to the interaction hamiltonian, respectively. We here consider only rotational transitions involving the rotational quantum numbers change $(J_{\rm i},M_{\rm i})\rightarrow(J_{\rm f},M_{\rm f})$ with $J_{\rm f}>J_{\rm i}$ (absorption) whose initial and final states are

$$\Psi_{\rm i}\left(\mathbf{R}_{\rm c},\mathbf{R},\mathbf{r}\right) = \Psi^{(\rm c)}\left(\mathbf{R}_{\rm c}\right)\Psi^{(\rm e)}\left(\mathbf{R},\mathbf{r}\right)\Psi^{(\rm N)}_{n,J_{\rm i},M_{\rm i}}\left(\mathbf{R}\right),$$
$$\Psi_{\rm f}\left(\mathbf{R}_{\rm c},\mathbf{R},\mathbf{r}\right) = \Psi^{(\rm c)}\left(\mathbf{R}_{\rm c}\right)\Psi^{(\rm e)}\left(\mathbf{R},\mathbf{r}\right)\Psi^{(\rm N)}_{n,J_{\rm f},M_{\rm f}}\left(\mathbf{R}\right). \quad (62)$$

where the center of the mass wave fuction $\Psi^{(\rm c)}\left(\mathbf{R}_{\rm c}\right)$ is highly localized at $\mathbf{R}_0$, $\Psi^{(\rm e)}\left(\mathbf{R},\mathbf{r}\right)$ is the electronic ground state and n is a vibrational quantum number which does not change. The transition probability is proportional to $\left|M_{\rm fi}\right|^2$ where the matrix element

$$M_{\rm fi}=\left\langle\Psi_{\rm f}\right|H_{\rm I}\left|\Psi_{\rm i}\right\rangle=\int d^3\mathbf{R}_{\rm c}\int d^3\mathbf{r}\int d^3\mathbf{R}\;\Psi_f^*\left(\mathbf{R}_{\rm c},\mathbf{R},\mathbf{r}\right)H_{\rm I}\left(\mathbf{R}_{\rm c},\mathbf{R},\mathbf{r}\right)\Psi_{\rm i}\left(\mathbf{R}_{\rm c},\mathbf{R},\mathbf{r}\right), \quad (63)$$

after exploiting the fact that the center of the mass of the molecule is practically located at $\mathbf{R}_0$, can be written as

$$M_{\rm fi}=\int d^3\mathbf{R}\left[\int d^3\mathbf{r}\;\left|\Psi^{(\rm e)}\left(\mathbf{R},\mathbf{r}\right)\right|^2 H_{\rm I}^{(\rm e)}\left(\mathbf{R}_0,\mathbf{r}\right)+\;H_{\rm I}^{(\rm N)}\left(\mathbf{R}_0,\mathbf{R}\right)\right]\Psi^{(\rm N)*}_{n,J_{\rm f},M_{\rm f}}\left(\mathbf{R}\right)\Psi^{(\rm N)}_{n,J_{\rm i},M_{\rm i}}\left(\mathbf{R}\right). \quad (64)$$

Quadrupolar absorption. The interaction Hamiltonian of Eq.(60) allows in principle to evaluate the matrix element $M_{\rm fi}$ in the presence of any radiation field and this is particularly suitable in the situation we are considering where the scattered field has deep-subwavelength spatial features. For very large molecules, the field has a remarkable spatial variation on the molecule volume and generally the standard multipole expansion of the interaction hamiltonian can not be approximated by only the dipole term. The molecular hydrogen ion we are investigating here is, on the other hand, the smallest molecule in nature so that its absorbtion spectroscopy can be analyzed by resorting to the multipolar expansion, but two observations are in order. In first place, this approach may fail if the molecule is close to the inner edge of the graphene ring where, as above detailed, the scattered field has spatial features of the order of the molecule length. Second, even though the approach is traditional, it nonetheless entails a dramatic enhancement of the absorption probability which unveils novel and viable absorption spectroscopy methods.

In order to perform the multipole expansion of the interaction hamiltonian of Eq.(60) we note that, as it is well known, the hydrogen molecular ion has no permanent dipole and hence the field has to be at least be expanded up the first order around the molecule center of the mass. Therefore, exploiting the Taylor expansions

$$\mathbf{E}\left(\mathbf{R}_0+u\mathbf{r}\right) = \mathbf{E}\left(\mathbf{R}_0\right)+u\left(\partial_iE_j\right)_{\mathbf{R}_0}x_i\hat{\mathbf{e}}_j,$$
$$\mathbf{E}\left(\mathbf{R}_0\pm\frac{1}{2}u\mathbf{R}\right) = \mathbf{E}\left(\mathbf{R}_0\right)\pm\frac{1}{2}u\left(\partial_iE_j\right)_{\mathbf{R}_0}X_i\hat{\mathbf{e}}_j, \quad (65)$$

where $\mathbf{r}=x_i\hat{\mathbf{e}}_i$, $\mathbf{R}=X_i\hat{\mathbf{e}}_i$ and $\mathbf{E}=E_i\hat{\mathbf{e}}_i$ are vector cartesian expansions, Eqs.(61) yield

$$H_{\rm I}^{(\rm e)}\left(\mathbf{R}_0,\mathbf{r}\right) = \frac{e}{2}\mathbf{r}\cdot\mathbf{E}\left(\mathbf{R}_0\right)+\frac{e}{4}\left(\partial_iE_j\right)_{\mathbf{R}_0}x_ix_j,$$
$$H_{\rm I}^{(\rm N)}\left(\mathbf{R}_0,\mathbf{R}\right) = -\frac{e}{8}\left(\partial_iE_j\right)_{\mathbf{R}_0}X_iX_j \quad (66)$$

and, consequently, Eq.(64) becomes

$$M_{\rm fi}=\int d^3\mathbf{R}\frac{e}{8}\left(\partial_iE_j\right)_{\mathbf{R}_0}\left[2\int d^3\mathbf{r}\;\left|\Psi^{(\rm e)}\left(\mathbf{R},\mathbf{r}\right)\right|^2 x_ix_j-X_iX_j\right]\Psi^{(\rm N)*}_{n,J_{\rm f},M_{\rm f}}\left(\mathbf{R}\right)\Psi^{(\rm N)}_{n,J_{\rm i},M_{\rm i}}\left(\mathbf{R}\right) \quad (67)$$

where we have used the fact that the electron provides no dipole contribution, i.e. $\int d^3\mathbf{r}\;\left|\Psi^{(\rm e)}\left(\mathbf{R},\mathbf{r}\right)\right|^2\mathbf{r}=0$ (since $\left|\Psi^{(\rm e)}\left(\mathbf{R},\mathbf{r}\right)\right|^2$ is spatially even while $\mathbf{r}$ is odd). The integration on the electron position $\mathbf{r}$ in Eq.(67) can be dealt with

by noting that, exploiting the rotational invariance of the electronic orbital $\left|\Psi^{(\mathrm{e})}(\mathbf{R},\mathbf{r})\right|^2$ around the internuclear vector $\mathbf{R}$, it is simple to prove that

$$\int d^3\mathbf{r}\,\left|\Psi^{(\mathrm{e})}(\mathbf{R},\mathbf{r})\right|^2 x_i x_j = a(R)\,\delta_{ij} + b(R)\,X_i X_j \tag{68}$$

where

$$\begin{aligned} a(R) &= \int d^3\mathbf{r}\,\left|\Psi^{(\mathrm{e})}(\mathbf{R},\mathbf{r})\right|^2 \frac{1}{2}\left[r^2 - \left(\hat{\mathbf{R}}\cdot\mathbf{r}\right)^2\right], \\ b(R) &= \int d^3\mathbf{r}\,\left|\Psi^{(\mathrm{e})}(\mathbf{R},\mathbf{r})\right|^2 \frac{1}{2}\left[3\left(\hat{\mathbf{R}}\cdot\mathbf{r}\right)^2 - r^2\right] \end{aligned} \tag{69}$$

are functions of only the internuclear distance $R=\sqrt{X^2+Y^2+Z^2}$. Inserting Eq.(68) into Eq.(67) and using the divergenceless of the scattered field ($0=\nabla\cdot\mathbf{E}=\partial_i E_i$) we get

$$M_{\mathrm{fi}} = \int d^3\mathbf{R}\frac{e}{8}\left[2b(R)-1\right]\left[\left(\partial_i E_j\right)_{\mathbf{R}_0}\left(X_iX_j - \frac{1}{3}\delta_{ij}R^2\right)\right]\Psi^{(\mathrm{N})*}_{n,J_{\mathrm{f}},M_{\mathrm{f}}}(\mathbf{R})\,\Psi^{(\mathrm{N})}_{n,J_{\mathrm{i}},M_{\mathrm{i}}}(\mathbf{R}), \tag{70}$$

clearly showing the quadrupolar nature of the interaction we are considering. In order to evaluate this integral, it is convenient to resort to the spherical tensor formalism which can here be set up by resorting to the relation (which is easy to check)

$$\left(\partial_i E_j\right)_{\mathbf{R}_0}\left(X_iX_j - \frac{1}{3}\delta_{ij}R^2\right) = \sqrt{\frac{4\pi}{15}}\sum_{q=-2}^{2} R^2 Y_2^q(\Theta,\Phi)\,V^q(\mathbf{R}_0) \tag{71}$$

where

$$\begin{aligned} V^2 &= \sqrt{2}\left(\hat{\mathbf{e}}_{\mathrm{R}}\cdot\nabla E_{\mathrm{L}}\right), \\ V^1 &= -\left(\hat{\mathbf{e}}_z\cdot\nabla E_{\mathrm{L}} + \hat{\mathbf{e}}_{\mathrm{R}}\cdot\nabla E_z\right), \\ V^0 &= -\sqrt{3}\left(\hat{\mathbf{e}}_{\mathrm{L}}\cdot\nabla E_{\mathrm{L}} + \hat{\mathbf{e}}_{\mathrm{R}}\cdot\nabla E_{\mathrm{R}}\right), \\ V^{-1} &= \left(\hat{\mathbf{e}}_z\cdot\nabla E_{\mathrm{R}} + \hat{\mathbf{e}}_{\mathrm{L}}\cdot\nabla E_z\right), \\ V^{-2} &= \sqrt{2}\left(\hat{\mathbf{e}}_{\mathrm{L}}\cdot\nabla E_{\mathrm{R}}\right), \end{aligned} \tag{72}$$

are the five spherical components of symmetric and traceless field gradient tensor $\partial_i E_j$. Inserting Eq.(71) into Eq.(70), exploiting Eq.(55) and using polar coordinates to perform the integration we get

$$M_{\mathrm{fi}} = \left[\frac{e}{8}\sqrt{\frac{4\pi}{15}}\int_0^{+\infty} dR\,R^2\left[2b(R)-1\right]\left|G_n(R)\right|^2\right]\sum_{q=-2}^{2} V^q(\mathbf{R}_0)\int d\Omega\,Y_2^q(\Omega)\,Y_{J_{\mathrm{i}}}^{M_{\mathrm{i}}}(\Omega)\,Y_{J_{\mathrm{f}}}^{M_{\mathrm{f}}*}(\Omega). \tag{73}$$

The integral of the product of three spherical harmonics is a standard one [12]

$$\int d\Omega\,Y_{j_1}^{m_1}(\Omega)\,Y_{j_2}^{m_2}(\Omega)\,Y_{j_3}^{m_3*}(\Omega) = \sqrt{\frac{(2j_1+1)(2j_2+1)}{4\pi(2j_3+1)}}\,\langle j_1,j_2;0,0\mid j_3,0\rangle\,\langle j_1,j_2;m_1,m_2\mid j_3,m_3\rangle \tag{74}$$

where $\langle j_1,j_2;m_1,m_2\mid j_3,m_3\rangle$ are the Clebsch-Gordan coefficients, so that Eq.(73) becomes

$$M_{\mathrm{fi}}(\mathbf{R}_0) = I_{J_{\mathrm{i}},J_{\mathrm{f}};n}\sum_{q=-2}^{2}\langle 2,J_{\mathrm{i}};q,M_{\mathrm{i}}\mid J_{\mathrm{f}},M_{\mathrm{f}}\rangle\,V^q(\mathbf{R}_0) \tag{75}$$

where

$$I_{J_{\mathrm{i}},J_{\mathrm{f}};n} = \frac{e}{8\sqrt{3}}\,\langle 2,J_{\mathrm{i}};0,0\mid J_{\mathrm{f}},0\rangle\sqrt{\frac{2J_{\mathrm{i}}+1}{2J_{\mathrm{f}}+1}}\int_0^{+\infty} dR\,R^2\left[2B(R)-1\right]\left|G_n(R)\right|^2. \tag{76}$$

The properties of the Clebsch-Gordan coefficients imply that

$$\begin{array}{lll} \langle 2, J_{\rm i}; 0, 0 \mid J_{\rm f}, 0\rangle \neq 0 & \text{if} & \left\{ \begin{array}{l} J_{\rm f} - J_{\rm i} \text{ even} \\ |J_{\rm i} - 2| \leq J_{\rm f} \leq J_{\rm i} + 2 \end{array} \right. \\ \langle 2, J_{\rm i}; q, M_{\rm i} \mid J_{\rm f}, M_{\rm f}\rangle \neq 0 & \text{if} & \left\{ \begin{array}{l} |J_{\rm i} - 2| \leq J_{\rm f} \leq J_{\rm i} + 2 \\ M_{\rm f} - M_{\rm i} = q \end{array} \right. \end{array} \tag{77}$$

reproducing the well known quadrupole selection rule

$$\begin{aligned} \Delta J &= 0, \pm 2 \qquad (J_{\rm i} = 0 \to J_{\rm f} = 0 \ \text{ forbidden}), \\ \Delta M &= 0, \pm 1, \pm 2. \end{aligned} \tag{78}$$

From Eq.(75) it is evident that the transition $M_{\rm i} \to M_{\rm f} = M_{\rm i} + q$ is locally triggered by the component V^q of the field gradient. Resorting to Eq.(14) for evaluating the components V^q of Eqs.(72) for the field of Eq.(13), we get

$$\begin{aligned} V^2(r_\perp, \varphi, z) &= e^{-i\varphi}\left[\frac{\partial \tilde{E}_{\rm L}}{\partial r_\perp}\right], \\ V^1(r_\perp, \varphi, z) &= e^{i0\varphi}\left[-\frac{\partial \tilde{E}_{\rm L}}{\partial z} - \frac{1}{\sqrt{2}}\left(\frac{\partial}{\partial r_\perp} + \frac{1}{r_\perp}\right)\tilde{E}_z\right], \\ V^0(r_\perp, \varphi, z) &= e^{i\varphi}\sqrt{\frac{3}{2}}\left[-\frac{\partial \tilde{E}_{\rm L}}{\partial r_\perp} - \left(\frac{\partial}{\partial r_\perp} + \frac{2}{r_\perp}\right)\tilde{E}_{\rm R}\right], \\ V^{-1}(r_\perp, \varphi, z) &= e^{i2\varphi}\left[\frac{\partial \tilde{E}_{\rm R}}{\partial z} + \frac{1}{\sqrt{2}}\left(\frac{\partial}{\partial r_\perp} - \frac{1}{r_\perp}\right)\tilde{E}_z\right], \\ V^{-2}(r_\perp, \varphi, z) &= e^{i3\varphi}\left[\left(\frac{\partial}{\partial r_\perp} - \frac{2}{r_\perp}\right)\tilde{E}_{\rm R}\right], \end{aligned} \tag{79}$$

showing that they have defined topological charge

$$V^q(r_\perp, \varphi, z) = \tilde{V}^q(r_\perp, z)\, e^{i(1-q)\varphi}. \tag{80}$$

Note that the impinging photons have angular momentum equal to $\hbar$ whereas also transition with angular momentum change $\hbar\Delta M = \pm 2\hbar$ are allowed, thus generally preventing the conservation of the projection along the z-axis of the total (radiation and matter) angular momentum. This is due to the fact that we have chosen for the quantization axis of the internuclear vector $\mathbf{R}$ the line parallel to z axis and passing through $\mathbf{R}_0$. Now the field is rotationally invariant only around the z-axis (passing thorough the center of the ring) and hence the conservation of total angular momentum is not guaranteed if the molecule is out of this axis. On the other hand if the molecule is on the z-axis ($\mathbf{R}_0 = Z_0\hat{\mathbf{e}}_z$) it is simple to prove that all the components $V^q(0, \varphi, Z_0)$ vanish except $V^1(0, \varphi, Z_0)$ (as it also obvious from the fact that V^1 is the only component with vanishing topological charge) so that only transition with $\Delta M = 1$ occurs, thus satisfying the conservation of the total angular momentum z-component.

Rotational absorption spettroscopy of molecular hydrogen ions. The above treatment of quadrupolar absorption of photons from molecular hydrogen ions is usually not considered in standard rotational spectroscopy since the available field gradients are generally too small to provide detectable absorption cross-sections. However, the above discussed field resonantly scattered by the graphene ring has deep-subwavelength spatial features, evidently entailing very large values of the field gradient. In order to show that such a field can actually make feasible rotational spectroscopy we compare the rotational absorption cross-section in the presence of the graphene ring with the one produced by the impinging plane wave without the ring. From Eq.(57), in a rotational transition $J_{\rm i} \to J_{\rm f} = J_{\rm i} + 2$, the frequency ω of the absorbed photon is such that

$$\hbar\omega = E^{(\rm N)}_{n,J_{\rm f}} - E^{(\rm N)}_{n,J_{\rm i}} = 2B\,(2J_{\rm i} + 3)\,. \tag{81}$$

The probability that such frequency is actually absorbed is proportional to sum of the squared matrix elements $|M_{\rm fi}|^2$ over all the initial $M_{\rm i}$ (which are thermally equiprobable) and over all the allowed final $M_{\rm f}$. As a consequence the absorption cross-section of such transition is

$$\sigma_{\rm mol} = g \sum_{M_{\rm i}=-J_{\rm i}}^{J_{\rm i}} \sum_{M_{\rm f}=-J_{\rm i}-2}^{J_{\rm i}+2} |M_{\rm fi}|^2, \tag{82}$$

where g is a proportionality constant. Using Eq.(75) and exploiting the fact that only the term with $M_{\rm f} = M_{\rm i} + q$ contributes, we get

$$\sigma_{\rm mol}\left(r_\perp, z\right) = g\left|I_{J_{\rm i},J_{\rm i}+2;n}\right|^2 \sum_{q=-2}^{2} w_q^{(J_{\rm i})} \left|\tilde{V}^q\left(r_\perp, z\right)\right|^2 \tag{83}$$

where

$$w_q^{(J_{\rm i})} = \sum_{M_{\rm i}=-J_{\rm i}}^{J_{\rm i}} \left\langle 2, J_{\rm i}; q, M_{\rm i} \mid J_{\rm i}+2, M_{\rm i}+q\right\rangle^2. \tag{84}$$

In the absence of the graphene ring the molecule is exposed to the sole impinging plane wave $\mathbf{E}^{(\rm i)} = E_0 e^{ik_0 z}\hat{\mathbf{e}}_{\rm L}$ whose field gradient has the only not vanishing component $V^1 = -ik_0 E_0 e^{ik_0 z}$ and accordingly the absorption cross-section is in this situation

$$\sigma_{\rm vac} = g\left|I_{J_{\rm i},J_{\rm i}+2;n}\right|^2 w_1^{(J_{\rm i})}\left|k_0 E_0\right|^2. \tag{85}$$

The efficiency of the graphene ring of enhancing the rotational absorbtion cross-section of a molecule is hence quantified by the ratio

$$\frac{\sigma_{\rm mol}\left(r_\perp, z\right)}{\sigma_{\rm vac}} = \sum_{q=-2}^{2} \frac{w_q^{(J_{\rm i})}}{w_1^{(J_{\rm i})}} \left|\frac{\tilde{V}^q\left(r_\perp, z\right)}{k_0 E_0}\right|^2. \tag{86}$$

Supplementary References

[1] Castro Neto, A. H., Guinea, F., Peres, N. M. R., Novoselov, K. S., and Geim, A. K. The electronic properties of graphene. *Rev. Mod. Phys.* **81**, 109 – 162 (2009).

[2] Chen, C.-F., Park, C.-H., Boudouris, B. W., Horng, J., Geng, B., Girit, C., Zettl, A., Crommie, M. F., Segalman, R. A., Louie, S. G., and Wang, F. Controlling inelastic light scattering quantum pathways in graphene. *Nature* **471**, 617 – 620 (2011).

[3] Liu, H., Liu, Y., and Zhua, D. Chemical doping of graphene. *J. Mater. Chem.* **21**, 3335 – 3345 (2011).

[4] Bonaccorso, F., Sun, Z., Hasan, T., and Ferrari, A. C. Graphene photonics and optoelectronics. *Nat. Photon.* **4**, 611 – 622 (2010).

[5] García de Abajo, F. J. Graphene Plasmonics: Challenges and Opportunities. *ACS Photon.* **1**, 135 – 152 (2014).

[6] Wang, W., Apell, P., and Kinaret, J. Edge plasmons in graphene nanostructures. *Phys. Rev. B* **84**, 085423 (2011).

[7] Jackson, J. D. Classical Electrodynamics, John Wiley & Sons Inc. (1999).

[8] Messiah, A. Quantum Mechanics (Vol 2), North-Holland (1962).

[9] Ciattoni, A., Rizza, C., Lee, H. W. H., Conti, C., and Marini, A. PlasmonEnhanced Spin-Orbit Interaction of Light in Graphene. *Laser & Photon. Rev.* **12**, 1800140 (2018).

[10] Schwinger, J., Deraad Jr., L. L., Milton, K. A., Tsai, W., and Norton, J. Classical Electrodynamics, CRC Press (1998).

[11] Prudnikov, A. P., Brychkov, I. A., and Marichev, O. I. Integrals and Series: Special functions, CRC Press (1986).

[12] Bransden, B. H., and Joachain, C. J. Physics of atoms and molecules, Pearson Education Limited (2003).

[13] Cohen-Tannoudji, C., Dupont-Roc, J., and Grynberg, G. Photons and Atoms: Introduction to Quantum Electrodynamics, Wiley-VCH (1997).